

# FAPP2 is involved in the transport of apical cargo in polarized MDCK cells

Otilia V. Vieira, Paul Verkade, Aki Manninen, and Kai Simons

Max Planck Institute for Molecular Cell Biology and Genetics, 01307 Dresden, Germany

**P**hosphatidylinositol-4-phosphate (PI(4)P) is the main phosphoinositide in the Golgi complex and has been reported to play a pleiotropic role in transport of cargo from the trans-Golgi network to the plasma membrane (PM) in polarized Madin–Darby canine kidney (MDCK) cells. Overexpression of the chimeric fluorescent protein encoding the pleckstrin homology domain, which is specific for PI(4)P, inhibited both apical and basolateral transport pathways. The transport of apical

cargo from the Golgi was shown to be specifically decreased by adenovirus-mediated RNA interference directed against PI(4)P adaptor protein (FAPP) 2. FAPP1 depletion had no effect on transport. On the other hand, FAPP2 was not involved in the Golgi-to-PM transport of cargo that was targeted to the basolateral membrane domain. Thus, we conclude that FAPP2 plays a specific role in apical transport in MDCK cells.

## Introduction

MDCK cells have the ability to generate and maintain biochemically distinct apical and basolateral plasma membrane (PM) domains by polarized protein sorting (Mostov et al., 2000). Apical sorting has been proposed to be based on cargo recruitment into raft domains, whereas basolateral sorting mainly involves cargo capture by cytosolic adaptors (Bonifacino and Traub, 2003; Schuck and Simons, 2004; Simons and Vaz, 2004). In MDCK cells, the trans-Golgi network (TGN) appears to be a major sorting station for apical and basolateral biosynthetic cargo, although sorting may also take place in endosomes (Keller et al., 2001; Ang et al., 2004). After cargo sorting, apical and basolateral transport carriers move along microtubules to fuse with their respective PM domain.

The molecular machinery that is responsible for the generation of post-Golgi carriers is poorly understood. However, the involvement of a lipid-based machinery in TGN-to-PM transport is becoming substantiated (Yeaman et al., 2004). Phosphoinositides have emerged as important regulators of membrane trafficking. Specifically, phosphatidylinositol-4-phosphate (PI(4)P) is known to be involved in the transport of

newly synthesized proteins from the TGN to PM in yeast (Hama et al., 1999; Walch-Solimena and Novick, 1999; Audhya et al., 2000) as well as in mammalian cells (Wang et al., 2003; Godi et al., 2004). It is still not clear how PI(4)P regulates membrane trafficking, but it is thought to function in the recruitment of transport machinery. For instance, the adaptor complex AP1 and EpsinR, which are involved in TGN-to-endosome traffic, bind to PI(4)P (Mills et al., 2003; Wang et al., 2003). Recently, two novel PI(4)P-binding proteins, PI(4)P adaptor proteins (FAPP) 1 and 2, were implicated in TGN-to-PM transport of the vesicular stomatitis virus glycoprotein (VSVG) and of glycosaminoglycans in COS7 cells (Godi et al., 2004). These ubiquitously expressed cytosolic proteins have a pleckstrin homology (PH) domain at the amino terminus through which they directly bind to PI(4)P. Both FAPPs also have a proline-rich domain that potentially mediates protein–protein interactions. Interestingly, FAPP2 contains a putative glycolipid transfer motif at its carboxy terminus, making it an interesting candidate for a role in the apical transport pathway (Dowler et al., 2000; Godi et al., 2004).

The role of PI(4)P in regulating polarized sorting to the cell surface in the Golgi complex of epithelial cells is unclear. Previous work has demonstrated that altered PI(4)P metabolism differentially affects biosynthetic surface delivery in MDCK cells (Weisz et al., 2000; Bruns et al., 2002). To gain more insight into the mechanisms of polarized trafficking, we have addressed the functional role of PI(4)P, FAPP1, and FAPP2 in the delivery of biosynthetic cargo from the Golgi complex to the cell surface in polarized MDCK cells.

Correspondence to Kai Simons: simons@mpi-cbg.de

Abbreviations used in this paper: CMV, cytomegalo virus; DKD, double KD; EndoH, endoglycosidase H; FAPP, PI(4)P adaptor protein; GL, glycosylated; GPI, glycosylphosphatidylinositol; IF, immunofluorescence; KD, knockdown; PAO, phenylarsine oxide; PH, pleckstrin homology; PI(4)P, phosphatidylinositol-4-phosphate; PM, plasma membrane; RNAi, RNA interference; shRNA, short hairpin RNA; TGN, trans-Golgi network; VSVG, vesicular stomatitis virus glycoprotein.

The online version of this article contains supplemental material.

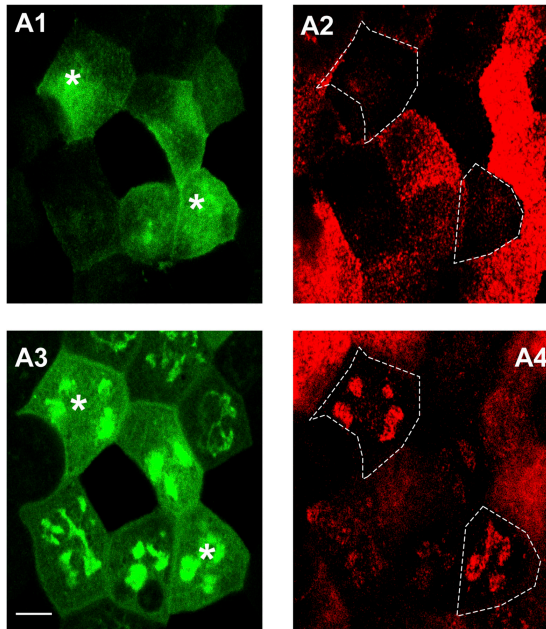


**Figure 1. YFP-PH overexpression blocks the Golgi-to-PM transport of newly synthesized HA in polarized MDCK cells.** (A1–A4) Polarized MDCK cells expressing YFP-PH for 14–16 h were infected with influenza virus. Cells were infected with influenza virus for 1 h, chased at 37°C for 2 h, and incubated at 20°C for 2 h. The cargo was released by incubating the cells at 37°C in the presence of cycloheximide for 30 min. (A1 and A2) Representative apical sections. (A3 and A4) Corresponding medial sections. The cells expressing PH domains (green) and HA (red) are outlined and indicated by asterisks. Bar, 10  $\mu\text{m}$ .

## Results and discussion

To find out whether PI(4)P potentially plays a role in post-Golgi transport in MDCK cells, we used the same strategy as Godi et al. (2004) and tested whether overexpression of PH domains would affect the transport of newly synthesized cargo. For that purpose, we constructed a fusion protein composed of a YFP and the PH domain of FAPP1 (YFP-PH). Polarized MDCK cells were infected with adenovirus to express the YFP-PH and were later infected with influenza virus to express HA as an apical cargo marker. In  $84.6 \pm 3.6\%$  (mean  $\pm$  SEM) of cells expressing YFP-PH, HA did not reach the apical membrane (Fig. 1, outlined cells and cells with asterisks) but colocalized with YFP-PH in the Golgi. In cells that expressed no or low levels of YFP-PH, HA transport to the apical membrane was unaffected (Fig. 1, cells without asterisks or outlines). The overexpression of PH domains also affected the basolateral transport of VSVG (BL-VSVG), a basolateral marker protein (Keller et al., 2001); in this study, the inhibitory effect was observed in  $65.3 \pm 4.2\%$  (mean  $\pm$  SEM) of cells. These results agree with a general role for PI(4)P in Golgi-to-PM delivery of cargo. This was also observed in nonepithelial cells, such as COS7 and HeLa cells (Wang et al., 2003; Godi et al., 2004), that use adaptors other than MDCK cells (Folsch et al., 2003; Wang et al., 2003; Ang et al., 2004) to send VSVG to the PM.

Among the known PI(4)P effectors, the FAPPs (FAPP1 and 2) are emerging as key players in post-Golgi traffic (Godi et al., 2004). Therefore, we studied their role in Golgi-to-PM transport in polarized MDCK cells. We generated adenoviruses

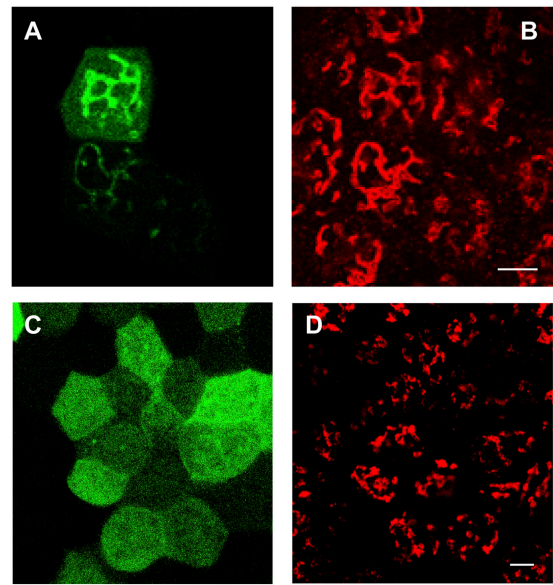


**Figure 2. Association of FAPP2 with the Golgi is PI(4)P dependent.** Fluorescence images of adenovirus-infected filter-grown MDCK cells expressing GFP-FAPP2 (green). GFP-FAPP2 distribution in control cells (A) and in cells treated with 10  $\mu\text{M}$  PAO during 15 min (C). (B and D) Golgi morphology revealed by giantin staining. Bars, 10  $\mu\text{m}$ .

expressing GFP fusion proteins of full-length FAPP1 and 2 to analyze their intracellular distribution. As seen in Fig. 2 (A and B), FAPP2 colocalized with giantin, suggesting a Golgi localization. The same result was obtained for FAPP1 (not depicted). The reduction of PI(4)P levels in MDCK cells using the phosphatidylinositol-4-kinase inhibitor phenylarsine oxide (PAO; Zheng and Bobich, 1998) at conditions in which no major morphological changes were observed abolished the association of FAPP2 with the Golgi (Fig. 2 C). This result clearly demonstrates that PI(4)P is necessary to target FAPPs to the Golgi in MDCK cells, as was shown previously in COS7 cells (Godi et al., 2004). It has also been shown that FAPP2 recruitment is dependent on ARF (ADP ribosylation factor) 1 (Godi et al., 2004), a small GTP-binding protein that is required for the recruitment of adaptor and coat proteins to the Golgi complex and TGN. We could see no effect of 5  $\mu\text{g/ml}$  Brefeldin A on the association of FAPP2 with the Golgi in MDCK cells (Ellis et al., 2004; unpublished data). However, the ARF–GTPase exchange factors that regulate ARF1 binding to the early Golgi in MDCK cells are insensitive to Brefeldin A treatment (Wagner et al., 1994); thus, these data do not rule out an involvement of ARF1 in FAPP2 function.

Next, the functional significance of FAPPs in polarized biosynthetic trafficking was assessed by RNA interference (RNAi). We initially used a retroviral RNAi system that was previously set up in our laboratory (Schuck et al., 2004). However, because this approach requires selection and culturing of MDCK cells before experiments, it might have been difficult to differentiate the effects of FAPP depletion on the polarization process in general from the specific effects on polarized transport. To restrict our focus on the biosynthetic sorting of proteins to the apical and basolateral PM domain, we constructed adenoviruses expressing short hairpin RNAs (shRNAs) target-

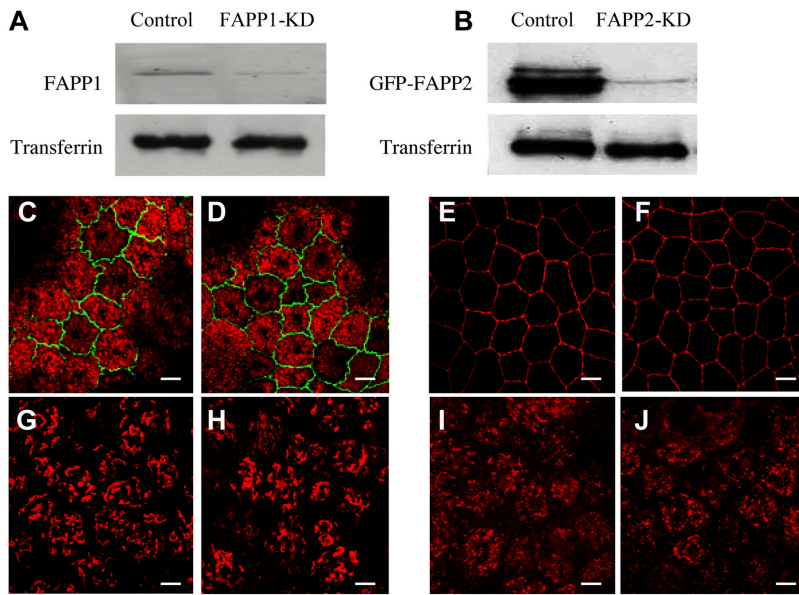


**Figure 3. Adenovirus-mediated RNAi KDs endogenous FAPP1 and 2 in polarized MDCK cells.** (A and B) Effect of RNAi on the protein levels of FAPP1 (A) and 2 (B). Cell lysates of MDCK cells 72 h after infection with empty virus (control) or with adenovirus-mediated RNAi were subjected to immunoblotting with anti-FAPP1, GFP, or transferrin receptor antibodies as a loading control. Fluorescence images showing the effect of simultaneous FAPP1 and 2 depletion (DKD cells) on the intracellular distribution of endogenous podocalyxin (C and D, red), ZO-1 (C and D, green), gp58 (E and F), giantin (G and H), and furin (I and J). (C, E, G, and I) Control cells. (D, F, H, and J) FAPP DKD cells. Bars, 10  $\mu$ m.

ing FAPP1 and 2. Adenovirus was chosen as the method of delivery of shRNAs to allow infection of filter-grown (already polarized) cells and, thereby, elucidate the effects of acute FAPP depletion specifically on polarized transport. 3 d after RNAi treatment, FAPP1 and 2 protein levels were measured by Western blot analysis (Fig. 3, A and B). The FAPP1 RNAi led to a drastic reduction in the level of FAPP1 protein (Fig. 3 A, second lane) when compared with control cells (Fig. 3 A, first lane). Because we did not have antibodies for FAPP2, we examined the effect of FAPP2 RNAi in cells expressing GFP-FAPP2 by using GFP antibodies and found that the expression levels of GFP-FAPP2 were efficiently reduced (Fig. 3 B, second lane). RT-PCR experiments confirmed that  $\sim 75$  and 80% of mRNA for FAPP1 and 2, respectively, were depleted in RNAi-treated cells. A coinfection of MDCK cells with FAPP1 and 2 knockdown (KD) adenoviruses (double KD [DKD]) resulted in similar KD efficiencies for individual FAPPs. Single and DKD cells were subjected to immunofluorescence (IF) to check whether the depletion of FAPPs affected the steady-state distribution of endogenous apical and basolateral markers. The polarized distribution of podocalyxin (apical), gp58 (basolateral), and ZO-1 (tight junctions) was unaffected in FAPP1 and 2 KDs as well as in DKD cells (Fig. 3, C–F). In addition, the depletion of FAPPs did not have any major effect on the morphology of Golgi or TGN as judged by giantin and furin staining, respectively (Fig. 3, G–J).

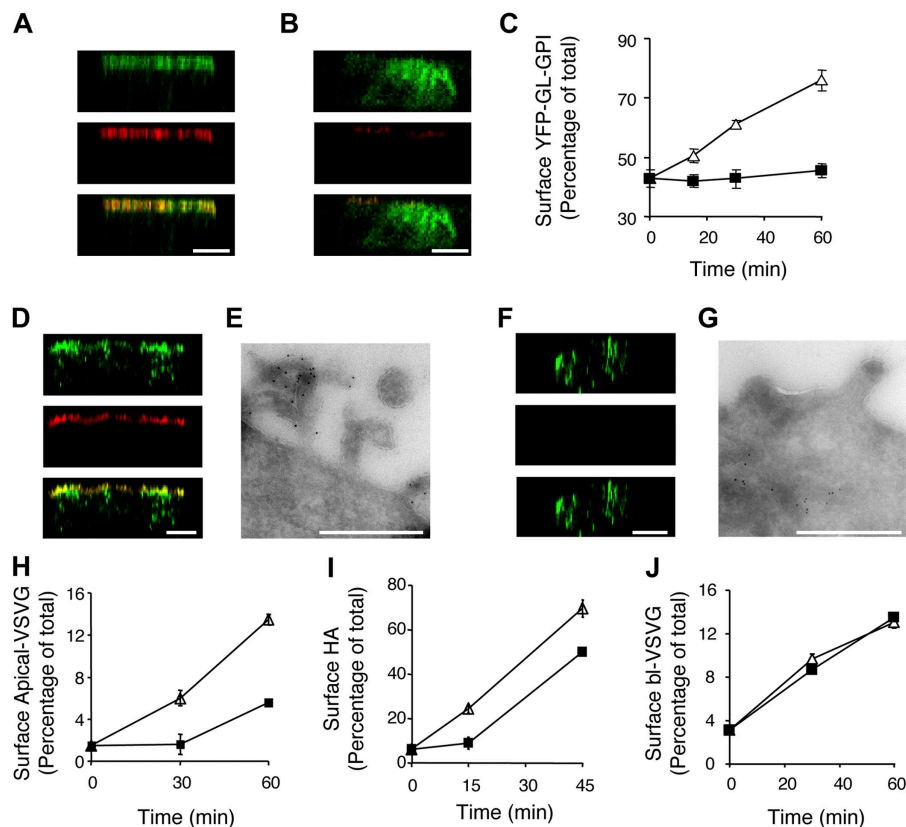
We then examined the biological role of FAPPs in polarized biosynthetic transport. The results depicted in Fig. 4 (A and B) and quantified (Fig. 4 C) by electrochemiluminescence showed that in DKD cells, the transport of YFP-glycosylated (GL) glycosylphosphatidylinositol (GPI) to the apical cell surface was inhibited. The transport of another apical membrane marker, a mutant of VSVG (A-VSVG), was also shown to be decreased in FAPP-depleted cells (Fig. 4, D–H). To examine the distribution of this apical cargo at the ultrastructural level, we performed EM immunocytochemistry on control and DKD cells. Although A-VSVG was observed on the PM and mi-

crovilli in control cells (Fig. 4 E), it was found in intracellular vesicles underneath the apical membrane in FAPP-depleted cells (Fig. 4 G). Quantitation of these data showed that in control cells,  $76 \pm 2\%$  (mean  $\pm$  SEM) of the gold particles was located at the PM, whereas it was only  $13 \pm 2\%$  in FAPP-depleted cells (*t* test,  $P < 0.0001$ ). Cell surface biotinylation confirmed these results (Fig. 4 H). Consistent with the above observations, HA transport to the cell surface was also affected by FAPP depletion (Fig. 4 I), although in this case, the inhibition was less dramatic. It should be pointed out that for all of the three apical cargos, the transport block could eventually be overcome with time, in part because we could not completely deplete the cell of FAPPs.

Finally, we examined the role of FAPPs in basolateral transport. No difference was seen in basolateral trafficking of BL-VSVG using confocal microscopy analysis (unpublished data). Cell surface biotinylation confirmed that in DKD cells, BL-VSVG was transported to the basolateral membrane with similar kinetics as observed in the control cells (Fig. 4 J). Altogether, our results show that FAPPs are part of the apical transport machinery. A noteworthy observation is that despite inhibition, we saw no evidence for the missorting of apical cargo to the basolateral side in FAPP-depleted MDCK cells (unpublished data).

To further characterize the individual roles of FAPP1 and 2 in the TGN-to-PM transport of apical cargo, we repeated the experiments with YFP-GL-GPI using FAPP1 or 2 single KD cells in comparison with DKD cells. This apical cargo was chosen because the effect of FAPP depletion on its transport to the PM was particularly striking, and its detection by electrochemiluminescence was very sensitive. Surprisingly, no effect was seen in FAPP1 KD cells. The transport of YFP-GL-GPI to the cell surface was inhibited to the same extent in FAPP2 depleted as it was in DKD cells (Fig. 5 A). The data so far suggest that the effect of FAPP2 on apical transport is on post-Golgi transport. To assess whether this was indeed the case, we analyzed the kinetics of ER-to-TGN transport of YFP-GL-GPI using en-

**Figure 4. FAPP depletion blocks apical but not basolateral cargo transport in polarized MDCK cells.** (A and B) Surface arrival of YFP-GL-GPI (red) was detected by GFP antibodies. Cells infected with empty adenovirus control (A) and with FAPP1 KD and FAPP2 KD adenoviruses (B). (C) Quantification of the effect of FAPP depletion on YFP-GL-GPI transport to the cell surface by electrochemiluminescence. (D–G) Cells expressing A-VSVG–GFP. (D and E) Control cells. (F and G) FAPP-depleted cells. (D and F) Cell surface VSVG labeling using an antibody against its ectodomain (red). (A, B, and D–G) Cargo was released for 30 min at 37 or 32°C, respectively. (E and G) EM analysis of A-VSVG–GFP. VSVG (12-nm gold) was localized to the microvilli (E) or to transport intermediates (G). Bars, 500 nm. (H) Cell surface biotinylation of A-VSVG in FAPP-depleted cells. (I) Effect of FAPP depletion on HA transport. (J) Quantification of the effect of FAPP depletion on BL-VSVG transport by cell surface biotinylation. Triangles, control; squares, cells coinfecting with adenoviruses to KD FAPP1 and 2. Data are means  $\pm$  SEM of three separate experiments.



doglycosidase H (EndoH) resistance pulse-chase experiments. YFP-GL-GPI became EndoH resistant with comparable kinetics in control and FAPP1 KD cells but not in FAPP2 KD cells (Fig. 5 B). However, the inhibitory effect on ER-to-TGN transport of YFP-GL-GPI that was caused by FAPP2 KD was small (15–20%) when compared with its TGN-to-PM transport (Fig. 5 A). It could be that this result reflects the requirement of FAPP2 for TGN release of cargo, which, in turn, may cause a delay in the ER-to-TGN transport (Fig. 5 B).

Recently, Polishchuk et al. (2004) reported that raft-associated GPI-anchored proteins are delivered to the basolateral surface and are rapidly transcytosed to the apical surface. However, in our experimental conditions, transcytosis of the newly synthesized YFP-GI-GPI only constituted a minor component in the biosynthetic transport of this apical cargo (Fig. S1, available at <http://www.jcb.org/cgi/content/full/jcb.200503078/DC1>). Thus, we suggest that FAPP2 depletion selectively affected the delivery of YFP-GL-GPI from the Golgi complex onwards.

The finding that cargo export from the Golgi to the apical PM was essentially normal in FAPP1 KD cells strongly suggests that the transport inhibition observed in FAPP2 KD cells was specific. Our attempts to rescue the FAPP2 KD phenotype by reexpressing an RNAi-resistant FAPP2 were unsuccessful as a result of the cytotoxic effects of even low levels of ectopic FAPP2 overexpression in MDCK cells.

Together, these data demonstrate that PI(4)P and FAPP2 are involved in the apical delivery machinery. Interestingly, FAPP2 could not be replaced by its close relative FAPP1. FAPP2 shares 90% similarity in its amino terminal region with FAPP1 but differs from it by having a carboxy-terminal exten-

sion. FAPP2's carboxy-terminal domain shows 98% sequence homology to glycolipid transfer proteins, which are cytosolic proteins that mediate the intermembrane transfer of glycolipids in vitro (Metz and Radin, 1980, 1982). Such an activity, once confirmed, would immediately suggest a function for FAPP2 in apical transport carrier formation.

Our working hypothesis for the segregation of apical from basolateral cargo in the Golgi is based on a raft-clustering mechanism in the TGN (Schuck and Simons, 2004). Sorting determinants on biosynthetic apical cargo would be recognized by sorting receptors that sequester cargo into the growing raft domain, which will form the apical carrier. Raft clustering is promoted by a reduction in line tension between the raft and nonraft phase. When an apical raft cluster has achieved a critical size, the line tension could overcome the energy required to bend the membrane, resulting in outward budding and release by fission between the phase boundaries. This process of domain-induced budding was first postulated on theoretical grounds and was recently experimentally verified in model systems (Baumgart et al., 2003).

In fact, YFP-GL-GPI associates with detergent-insoluble lipid microdomains in the Golgi complex after the addition of complex sugars. As shown in Fig. S2 (available at <http://www.jcb.org/cgi/content/full/jcb.200503078/DC1>), FAPP2 depletion changes YFP-GL-GPI insolubility in cold Triton X-100, and similar results were obtained regardless of whether the cells were chased for 1.5 or 3 h. The overall YFP-GL-GPI insolubility increased faster in control than in FAPP2 KD cells ( $89.3 \pm 6.6\%$  insoluble in control cells vs.  $55 \pm 5.6\%$  insoluble in FAPP2 KD cells;  $n = 3$ ). The results suggest that altered

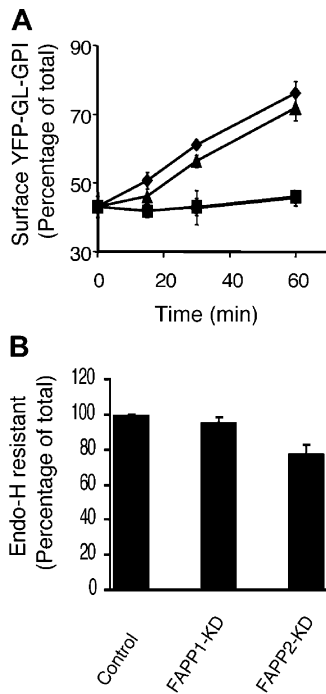


**Figure 5. FAPP2 but not FAPP1 is mainly responsible for the apical transport phenotype.** (A) Quantification of the effect of single KDs on YFP-GL-GPI transport to the cell surface by electrochemiluminescence. Diamonds, control; triangles, FAPP1 KD cells; circles, FAPP2 KD cells (overlaps with the DKD curve); squares, DKD cells. (B) Effect of FAPP1 and 2 KD on ER-to-Golgi transport of YFP-GL-GPI assessed by EndoH resistance. The amount of EndoH-resistant cargo in control cells after 1-h chase was set to 100%, and KD cell data are shown relative to that. Data are means  $\pm$  SEM of three separate experiments.

association of YFP-GL-GPI with lipid rafts may be responsible for the delay in transport that is observed in FAPP2 KD cells.

How could FAPP2 contribute to this process? First, by binding to PI(4)P, a Golgi landmark, correct subcellular location would be conferred. Second, by binding to glucosylceramide, which is the only known glycolipid that is synthesized in the cytoplasmic leaflet of the Golgi (Jeckel et al., 1992), FAPP2 could, by oligomerization, contribute to stabilization of the raft cluster. Third, via its proline-rich motif (Dowler et al., 2000), FAPP2 could bind to other components of the apical transport machinery. In such a scenario, FAPP2 would serve as a key regulator in the process. However, several issues still need experimental confirmation: FAPP2 binding to glucosylceramide, oligomerization upon binding, and the identification of possible binding partners.

## Materials and methods

### Reagents and antibodies

Cell culture media were from Invitrogen or PAA Laboratories. PAO was from Sigma-Aldrich. Antibodies against VSVG ectodomain and gp58 (Balcarova-Stander et al., 1984) have been raised in our lab. Other antibodies that were used are as follows: rabbit anti-ZO-1 and mouse antitransferrin receptor (Zymed Laboratories), rabbit antifurin (Affinity BioReagents, Inc.), mouse antigiantin (provided by H.P. Hauri, University of Basel, Basel, Switzerland), and goat anti-GFP (provided by D. Drechsel, Max Planck Institute, Dresden, Germany). Hybridoma cells producing the podocalyxin antibody were supplied by G. Ojakian (State University of New York Downstate Medical Center, Brooklyn, NY). FAPP1 antibody was

raised against the amino terminus of FAPP1 (VCKGSKGSIK). Fluorochrome-conjugated secondary antibodies were from Jackson ImmunoResearch Laboratories.

### Cell culture and adenovirus infection

MDCK cells were grown on transwell polycarbonate filters (Costar) in MEM with 10% FCS and were infected with adenoviruses as described previously (Keller et al., 2001). For RNAi experiments, filter-grown MDCK cells that were seeded 24 h before were infected for 3 h with the adenovirus-mediated RNAi. The cells were grown for 72 h more and were processed for IF or biochemical analysis.

### IF, confocal microscopy, and immuno-EM

IF was performed as described previously (Fullekrug et al., 1999). Fixed stained sample cells were analyzed by confocal microscopy using a laser scanning confocal microscope (model LSM510; Carl Zeiss MicroImaging, Inc.) with a 100 $\times$  oil immersion objective (Carl Zeiss MicroImaging, Inc.). Digital images were prepared using Adobe Photoshop and Adobe Illustrator.

Immuno-EM was performed as described previously (Scheiffele et al., 1998). Gold particles located between the nucleus and the apical PM were counted. Gold particles located within 25 nm of the apical PM were assigned as having reached the surface. Surface arrival was expressed as the number of gold particles at the PM divided by the total (PM + cytoplasm) number of gold particles multiplied by 100%. 10 cells of each group were quantitated.

### Constructs and generation of recombinant adenoviruses

The generation of the plasmids and adenovirus that were used for expression of YFP-GL-GPI and BL-VSVG were described previously (Keller et al., 2001). The generation of the A-VSVG construct is described in detail in the online supplemental material (available at <http://www.jcb.org/cgi/content/full/jcb.200503078/DC1>). YFP-PH was amplified by PCR using a plasmid encoding the chimera of YFP with PH domain (pYFP-C3; CLONTECH Laboratories, Inc.), which was provided by M. Zerial (Max Planck Institute). YFP-PH was then subcloned in pShuttle-cytomegalo virus (CMV) as a Sall-NotI fragment. The plasmids encoding the human full-length FAPP1 and 2 were provided by J. Lucocq (University of Dundee, Dundee, Scotland, UK). GFP-FAPP1 was amplified by PCR and was inserted into pShuttle-CMV as described above. FAPP2 was released from PEB62T vector as a BamHI fragment and was transferred into pEGFP-C1 (CLONTECH Laboratories, Inc.). GFP-FAPP2 was then amplified by PCR and subcloned into pShuttle-CMV as a NotI-XbaI fragment. For RNAi cloning, unique sequences conforming to AAN19 were selected, and the oligonucleotides encoding shRNAs directed against FAPP1 and 2 were designed and cloned into pSUPER as described previously (Schuck et al., 2004). The shRNA expression cassette was then transferred into the XhoI-NotI site of pShuttle. The propagation and generation of recombinant adenoviruses were performed as described in the pAdeasyTM vector protocol. All oligonucleotide sequences are supplied in the online supplemental material (available at <http://www.jcb.org/cgi/content/full/jcb.200503078/DC1>).

### EndoH digestion, surface biotinylation, and HA transport

Digestion with EndoH and cell surface biotinylation were performed as described previously (Keller et al., 2001). Surface arrival of HA was detected by trypsin cleavage as described previously (Keller and Simons, 1998).

### Quantification of cell surface arrival of YFP-GL-GPI by electrochemiluminescence

To quantify the arrival of YFP-GL-GPI at the cell surface and in order to distinguish the surface from the intracellular cargo, we took advantage of the existence of a trypsin cleavage site between the protein and GPI. The detection of fluorescence in trypsin solution and cell lysates was performed by electrochemiluminescence with ruthenylated polyclonal GFP antibodies. A detailed description of this method is provided in the online supplemental material (available at <http://www.jcb.org/cgi/content/full/jcb.200503078/DC1>).

### SDS-PAGE and immunoblotting

Cell lysates (prepared with lysis buffer containing protease inhibitors) were resolved by SDS-PAGE and transferred onto polyvinylidene difluoride membranes.

### Online supplemental material

Online supplemental Materials and methods describes the cloning of A-VSVG and provides other oligonucleotide sequences. It also describes the quantification of cell surface arrival of YFP-GL-GPI by electrochemiluminescence.

cence. Fig. S1 shows that FAPP2 depletion does not affect transcytosis. Fig. S2 shows that FAPP2 depletion affects the detergent solubility of YFP-GPI. Online supplemental material is available at <http://www.jcb.org/cgi/content/full/jcb.200503078/DC1>.

We thank C. Walch-Solimena, B. Hoflack, and members of the Simons lab for many helpful comments and S. Dienel for her technical assistance. We are indebted to P. Keller for his expertise on the electrochemiluminescence measurements.

O.V. Vieira is the recipient of a Marie Curie postdoctoral fellowship. A. Manninen is a recipient of the EMBO long-term fellowship. This work was supported by grants SFB-TR13-TPA1 and HPRN-CT-2002-00259.

Submitted: 15 March 2005

Accepted: 12 July 2005

## References

- Ang, A.L., T. Taguchi, S. Francis, H. Folsch, L.J. Murrells, M. Pypaert, G. Warren, and I. Mellman. 2004. Recycling endosomes can serve as intermediates during transport from the Golgi to the plasma membrane of MDCK cells. *J. Cell Biol.* 167:531–543.
- Audhya, A., M. Foti, and S.D. Emr. 2000. Distinct roles for the yeast phosphatidylinositol 4-kinases, Stt4p and Pik1p, in secretion, cell growth, and organelle membrane dynamics. *Mol. Biol. Cell.* 11:2673–2689.
- Balcarova-Stander, J., S.E. Pfeiffer, S.D. Fuller, and K. Simons. 1984. Development of cell surface polarity in the epithelial Madin-Darby canine kidney (MDCK) cell line. *EMBO J.* 3:2687–2694.
- Baumgart, T., S.T. Hess, and W.W. Webb. 2003. Imaging coexisting fluid domains in biomembrane models coupling curvature and line tension. *Nature.* 425:821–824.
- Bonifacino, J.S., and L.M. Traub. 2003. Signals for sorting of transmembrane proteins to endosomes and lysosomes. *Annu. Rev. Biochem.* 72:395–447.
- Bruns, J.R., M.A. Ellis, A. Jeromin, and O.A. Weisz. 2002. Multiple roles for phosphatidylinositol 4-kinase in biosynthetic transport in polarized Madin-Darby canine kidney cells. *J. Biol. Chem.* 277:2012–2018.
- Dowler, S., R.A. Currie, D.G. Campbell, M. Deak, G. Kular, C.P. Downes, and D.R. Alessi. 2000. Identification of pleckstrin-homology-domain-containing proteins with novel phosphoinositide-binding specificities. *Biochem. J.* 351:19–31.
- Ellis, M.A., M.T. Miedel, C.J. Guerriero, and O.A. Weisz. 2004. ADP-ribosylation factor 1-independent protein sorting and export from the trans-Golgi network. *J. Biol. Chem.* 279:52735–52743.
- Folsch, H., M. Pypaert, S. Maday, L. Pelletier, and I. Mellman. 2003. The AP-1A and AP-1B clathrin adaptor complexes define biochemically and functionally distinct membrane domains. *J. Cell Biol.* 163:351–362.
- Fullekrug, J., P. Scheiffele, and K. Simons. 1999. VIP36 localisation to the early secretory pathway. *J. Cell Sci.* 112:2813–2821.
- Godi, A., A. Di Campli, A. Konstantakopoulos, G. Di Tullio, D.R. Alessi, G.S. Kular, T. Daniele, P. Marra, J.M. Lucocq, and M.A. De Matteis. 2004. FAPPs control Golgi-to-cell-surface membrane traffic by binding to ARF and PtdIns(4)P. *Nat. Cell Biol.* 6:393–404.
- Hama, H., E.A. Schnieders, J. Thorner, J.Y. Takemoto, and D.B. DeWald. 1999. Direct involvement of phosphatidylinositol 4-phosphate in secretion in the yeast *Saccharomyces cerevisiae*. *J. Biol. Chem.* 274:34294–34300.
- Jeckel, D., A. Karrenbauer, K.N. Burger, G. van Meer, and F. Wieland. 1992. Glucosylceramide is synthesized at the cytosolic surface of various Golgi subfractions. *J. Cell Biol.* 117:259–267.
- Keller, P., and K. Simons. 1998. Cholesterol is required for surface transport of influenza virus hemagglutinin. *J. Cell Biol.* 140:1357–1367.
- Keller, P., D. Toomre, E. Diaz, J. White, and K. Simons. 2001. Multicolor imaging of post-Golgi sorting and trafficking in live cells. *Nat. Cell Biol.* 3:140–149.
- Metz, R.J., and N.S. Radin. 1980. Glucosylceramide uptake protein from spleen cytosol. *J. Biol. Chem.* 255:4463–4467.
- Metz, R.J., and N.S. Radin. 1982. Purification and properties of a cerebroside transfer protein. *J. Biol. Chem.* 257:12901–12907.
- Mills, I.G., G.J. Praefcke, Y. Vallis, B.J. Peter, L.E. Olesen, J.L. Gallop, P.J. Butler, P.R. Evans, and H.T. McMahon. 2003. EpsinR: an AP1/clathrin interacting protein involved in vesicle trafficking. *J. Cell Biol.* 160:213–222.
- Mostov, K.E., M. Verges, and Y. Altschuler. 2000. Membrane traffic in polarized epithelial cells. *Curr. Opin. Cell Biol.* 12:483–490.
- Polishchuk, R., A. Di Pentima, and J. Lippincott-Schwartz. 2004. Delivery of raft-associated, GPI-anchored proteins to the apical surface of polarized MDCK cells by a transcytotic pathway. *Nat. Cell Biol.* 6:297–307.
- Scheiffele, P., P. Verkade, A.M. Fra, H. Virta, K. Simons, and E. Ikonen. 1998. Caveolin-1 and -2 in the exocytic pathway of MDCK cells. *J. Cell Biol.* 140:795–806.
- Schuck, S., and K. Simons. 2004. Polarized sorting in epithelial cells: raft clustering and the biogenesis of the apical membrane. *J. Cell Sci.* 117:5955–5964.
- Schuck, S., A. Manninen, M. Honsho, J. Fullekrug, and K. Simons. 2004. Generation of single and double knockdowns in polarized epithelial cells by retrovirus-mediated RNA interference. *Proc. Natl. Acad. Sci. USA.* 101:4912–4917.
- Simons, K., and W.L. Vaz. 2004. Model systems, lipid rafts, and cell membranes. *Annu. Rev. Biophys. Biomol. Struct.* 33:269–295.
- Wagner, M., A.K. Rajasekaran, D.K. Hanzel, S. Mayor, and E. Rodriguez-Boulan. 1994. Brefeldin A causes structural and functional alterations of the trans-Golgi network of MDCK cells. *J. Cell Sci.* 107:933–943.
- Walch-Solimena, C., and P. Novick. 1999. The yeast phosphatidylinositol-4-OH kinase pik1 regulates secretion at the Golgi. *Nat. Cell Biol.* 1:523–525.
- Wang, Y.J., J. Wang, H.Q. Sun, M. Martinez, Y.X. Sun, E. Macia, T. Kirchhausen, J.P. Albanesi, M.G. Roth, and H.L. Yin. 2003. Phosphatidylinositol 4 phosphate regulates targeting of clathrin adaptor AP-1 complexes to the Golgi. *Cell.* 114:299–310.
- Weisz, O.A., G.A. Gibson, S.M. Leung, J. Roder, and A. Jeromin. 2000. Overexpression of frequenin, a modulator of phosphatidylinositol 4-kinase, inhibits biosynthetic delivery of an apical protein in polarized Madin-Darby canine kidney cells. *J. Biol. Chem.* 275:24341–24347.
- Yeaman, C., M.I. Ayala, J.R. Wright, F. Bard, C. Bossard, A. Ang, Y. Maeda, T. Seufferlein, I. Mellman, W.J. Nelson, and V. Malhotra. 2004. Protein kinase D regulates basolateral membrane protein exit from trans-Golgi network. *Nat. Cell Biol.* 6:106–112.
- Zheng, X., and J.A. Bobich. 1998. A sequential view of neurotransmitter release. *Brain Res. Bull.* 47:117–128.